

Design and Analysis of Rotating Detonation Wave Engine



V. Ramanujachari, Rahul Dutta Roy, and P. Amrutha Preethi

Abstract Rotating detonation wave engine (RDE) would be the futuristic engine for air-breathing missile systems and gas turbine systems (aero and stationary applications). The continuous operation of RDE with an operating frequency of 3–15 kHz is attractive for propulsion systems based on rocket, ramjet and turbojet engines. The cell size is the characteristic dimension of the cellular pattern of a propagating detonation wave. The cell size is found to depend strongly on the choice of fuel and oxidizer, its equivalence ratio, initial temperature and initial pressure. Some empirical relations based on cell size are used to design the present detonation combustor. Hydrogen is chosen as the fuel, while air is selected as the oxidizer. The RDE hardware has been realized, and the test facility is being modified at NCCRD, IIT, Madras to carry out static tests. The analysis of the RDE combustor without the nozzle is carried out using the “pressure history model” reported in literature. As the hydrogen fuel and air are entering as two different streams perpendicular to each other, a simple mixing analysis has been carried out to evaluate the mixture properties ahead of the detonation wave. The Chapman–Jouguet (CJ) detonation computations are carried out using the detonation tool box runs in conjunction with Cantera software assuming chemical equilibrium. The fuel-based specific impulse resulted from the present analysis for our configuration using H₂–air is 4733 s compared to a value of 4706 s reported in literature for a stoichiometric composition. The same model has been used to evaluate the C₂H₄–air system. The specific impulse of our study is 2111 s compared to 1975s reported in literature for the fuel-based equivalence ratio of 0.5. This has given credence to the results of the analytical work.

Keywords Rotating detonation wave engine · Pressure history model · CJ detonation · Specific thrust · Specific impulse

V. Ramanujachari (✉) · R. Dutta Roy
National Centre for Combustion Research and Development, IIT Madras, Chennai 600036, India
e-mail: vramanujachari@yahoo.co.in

P. Amrutha Preethi
G. Pulla Reddy Engineering College, Kurnool 518007, India

Nomenclature

A	Area (m^2)
F	Force (N)
H	Mixture layer height (m)
K	Value of integral
P	Pressure (bar)
P_a	Ambient pressure (bar)
\bar{P}_c	Average pressure acting on the thrust surface
\bar{R}	Mean radius of combustion chamber (m)
S	Surface area (m^2)
T	Temperature (K)
V	Velocity (m/s)
W, w	Width of the annular space (m)
X	Azimuthal coordinate
Z, x	Axial coordinate
c_p	Specific heat at constant pressure (J/Kg-K)
h	Enthalpy (MJ/kg)
\dot{m}	Mass flow rate
p	Static pressure (bar)
t	Time (ms)
u	Velocity (m/s)

Greek Symbols

ρ	Density (kg/m^3)
γ	Ratio of specific heats
γ_e	Ratio of specific heats at equilibrium condition
τ_w	Shear stress on the walls (N/m^2)

Subscripts

1	Airflow state
2	Fuel flow state
3	Mixture state
c	Averaged combustion chamber conditions

1 Introduction

The rotating detonation wave engine has emerged as a promising concept due to its high specific power output, thrust to weight ratio and volumetric efficiency [1]. This has been proposed as a substitute for liquid propellant rocket or ramjet/engine [2]. In addition, it can replace gas turbine engines for power generation also [3]. Due to its promising potential as a propulsive and power generation device, it has been researched worldwide based on both numerical and experimental investigations. It has been reported that the detonation wave propagates with high velocity deficit when compared to CJ detonation wave velocity [3]. A lot of countries abroad are working on this concept. In order to understand this RDE and realize an engine to deliver adequate thrust, an experimental work has been initiated. An experimental engine is designed based on the empirical correlations of Bykovskii et al. [4] by the authors at IIT, Madras, [5] and the hardware is being tested. In the present work, it is analysed to obtain the performance of the engine using simple one-dimensional modelling technique. Davidenko et al. [6], Shepherd and Kasahara [7] and Braun [8] have carried out simple modelling of the complex detonation wave phenomena. Universal relationship, based on experimental data on expansion wave pressures downstream of detonation front was evolved by Sichel and Foster [9]. This has been used as a part of the performance prediction method. The objective of this paper is to show how an engine analysis can be carried out for an engine designed based on empirical methods. Hence, no parametric study is reported. This work establishes the conditions to be set for the proposed experiments and the performance expected from the engine tests.

2 Concept of RDE

In RDE concept, a unidirectional detonation wave could be created and the exhaust gases are expanded through an annular nozzle producing necessary thrust. Figure 1 shows the elements of a rotating detonation wave engine concept designed and realized by the authors. In this case, the combustor or the detonation chamber is the annular ring, where the premixed fuel-air mixture is prepared for detonation by injecting axially the hydrogen fuel and radially the air at the one end of the combustor. After initiation of combustion, a detonation wave propagates circumferentially around the annular ring near the plane of the injector. The detonation products are expanded and exhausted out of the other end of the combustor, which could have a nozzle to further increase the thrust. RDE provides steady source of thrust without needing initiation for every cycle. In RDE, the detonable mixture is injected axially and the detonation wave runs circumferentially around the annular combustor making the flow field very complex, leading to the design very difficult. In addition, as the detonation wave is continuously rotating in a particular location

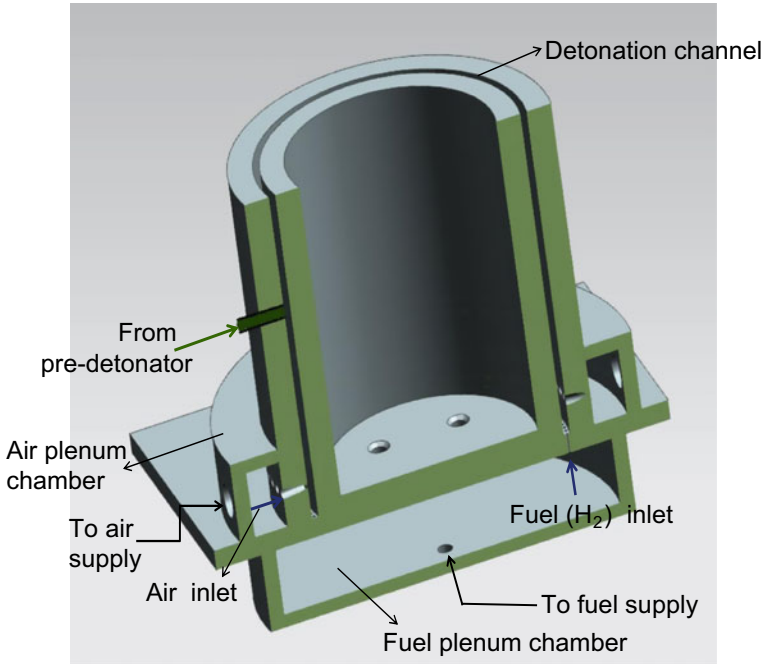


Fig. 1 Elements of a rotating detonation engine

inside the combustion chamber, the heat transfer to the wall and its control would be a major challenge.

As the radial dimension of the RDE is very small compared to the azimuthal and axial dimensions, the variation of flow properties in the radial direction can be considered negligible. The modelling of the flow field behind the detonation wave is quite complex due to oblique shock wave, contact surface between combustion products of detonation wave and shocked combustion products and the expansion waves. Hence, the RDE is “unrolled” into two-dimension as shown in Fig. 2 to make it amenable for simple computations.

3 Pressure History Model of RDE

It is assumed that the fuel and oxidizer are well mixed and supplied at a constant average mass flow rate. The detonation wave propagates at a constant speed equal to CJ detonation speed. The second assumption is that the flow properties are periodic with a period of T (inverse of frequency).

This implies that the flow would be steady in a frame co-rotating with the detonation wave. The third assumption is that the radial variation in the flow may be

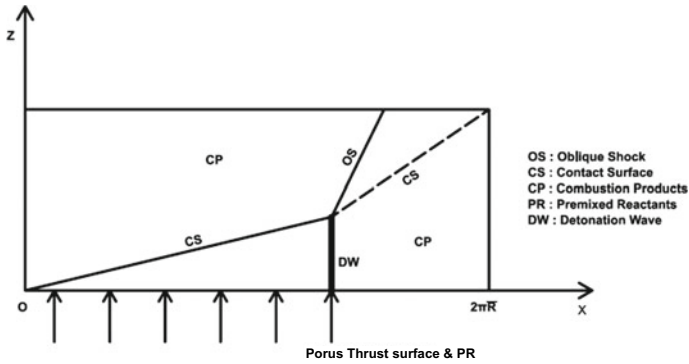


Fig. 2 Unwrapped flow field of RDE

neglected and the flow can be approximated as two-dimensional flow in space. It is reported that the two-dimensional models are adequate for computing average thrust [7]. By averaging over a period, the azimuthal and time dependence of the flow can be eliminated for computing the propulsion parameters. This gives the simplification that the modelling can be quasi one-dimensional and the properties depend on axial direction, Z only. Figure 3 shows the control volume considered for the pressure history model [7]. This encloses the engine but does not cross the exit plane. Here, the control volume is placed along the walls of the combustion chamber and crosses the inlet plane of the combustion chamber. This enables the computation of thrust based on the condition at the porous thrust surface. The forces in the axial direction for this control volume are given below:

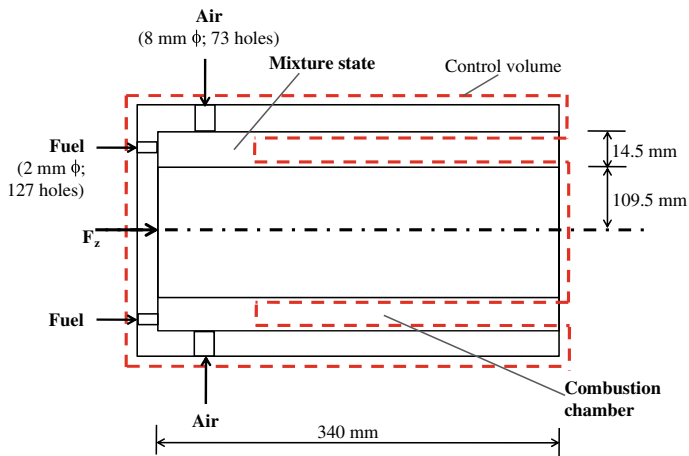


Fig. 3 Control volume for the pressure history model postulated by Shepherd and Kasahara [7]

$$F_Z = \underbrace{\int_{A_c} (P_c - P_{c,1}) dS}_I + \underbrace{\int_{A_c} [\rho_c u_{z,c}^2 + (P_{c,1} - P_a)] dS}_II - \underbrace{\int_{A_w} \tau_w dS}_III \quad (1)$$

First term in the above equation represents the integrated effects of the detonation generated pressure force on the injector surface at the upstream end of the combustion chamber. This can be expressed as

$$F_I = A_c (\bar{P}_c - P_{c,1}) \quad (2)$$

Here, the averaged pressure \bar{P}_c has to be computed. The second term represents the force associated with the momentum flux of the gas at the inlet to the combustion chamber. This can be expressed as

$$F_{II} \approx A_c (P_{c,1} - P_a) + \bar{u}_c \dot{m} \quad (3)$$

Here, the averaged velocity is obtained based on the mass continuity equation. The third term represents the friction due to viscous forces on the combustion chamber walls. This can be neglected and compared to the magnitudes of the first two terms.

4 Modelling of Injection Process

It is essential to obtain an injection model just upstream of the detonation for subsequent modelling based on pressure history model. For simplicity, one-dimensional steady flow equations of continuity, momentum and energy are formulated and solved to obtain the mixture properties of fuel and air prior to detonation in the annular combustor. State 1 is for the air flow; state 2 is for the fuel flow, and state 3 for the mixture conditions. In all the cases, the total pressure of the air is maintained at 4.5 bar(abs) and hence, the flow rate of air is constant at 3.852 kg/s. Depending upon the fuel-based equivalence ratio, the fuel flow rate is varied. As the number and diameter of the fuel injection holes are fixed, the fuel injection total pressure is varied to allow the required amount of fuel flow as shown in Fig. 4.

1. Continuity equation

$$\dot{m}_1 + \dot{m}_2 = \dot{m}_3 \quad (4)$$

$$\dot{m}_3 = \rho_3 A_3 V_3 \quad (5)$$

2. Energy equation

$$\frac{\dot{m}_1}{\dot{m}_3} \left(h_1 + \frac{V_1^2}{2} \right) + \frac{\dot{m}_2}{\dot{m}_3} \left(h_2 + \frac{V_2^2}{2} \right) = c_{p,3} T_3 + \frac{V_3^2}{2} \quad (6)$$

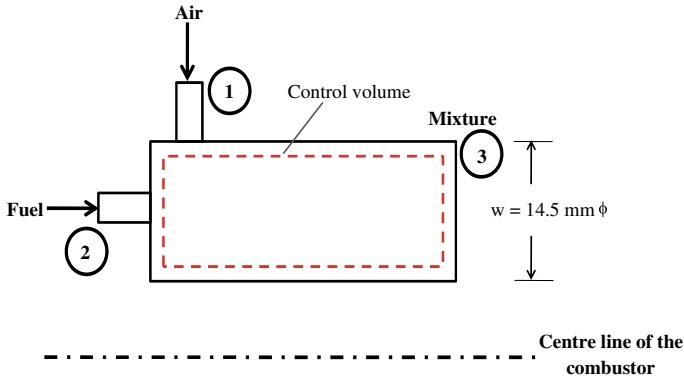


Fig. 4 Control volume for the injection process

3. Axial momentum equation

$$\dot{m}_2 V_2 + p_2 A_2 + p_1 (A_3 - A_2) = \dot{m}_3 V_3 + p_3 A_3 \tag{7}$$

The axial momentum contribution of air flow is not considered as air is injected perpendicular to the axial direction. We have three equations and three unknowns (p_3, T_3, V_3). These equations can be solved using Newton–Raphson method. We can use isentropic equations to obtain the stagnation pressure, stagnation temperature and Mach number at the mixture state. Figures 5, 6, 7 and 8 show the distribution of mass flow rate of fuel, Mach number, total and static pressures and total and static temperatures of the mixtures. As the mass flow rate of air is kept constant for all the fuel-based equivalence ratios, the fuel flow rate continuously increases with increase in equivalence ratio as shown in Fig. 5.

The Mach number of the mixture over the range of equivalence ratios is shown in Fig. 6. A slight decrease in trend is noted. This may be due to the particular gas constant effect of the hydrogen air mixture, which in turn affects the sonic speed of the mixture. The sonic speed marginally increases due to the mixture ratio

Fig. 5 Mass flow rate of fuel versus equivalence ratio

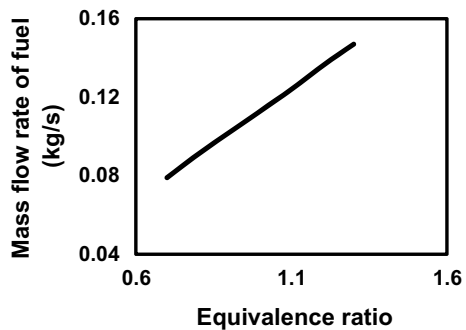


Fig. 6 Mach number versus equivalence ratio

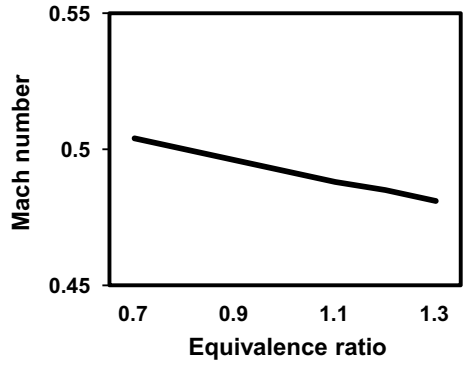


Fig. 7 Total and static pressure of reactants versus equivalence ratio

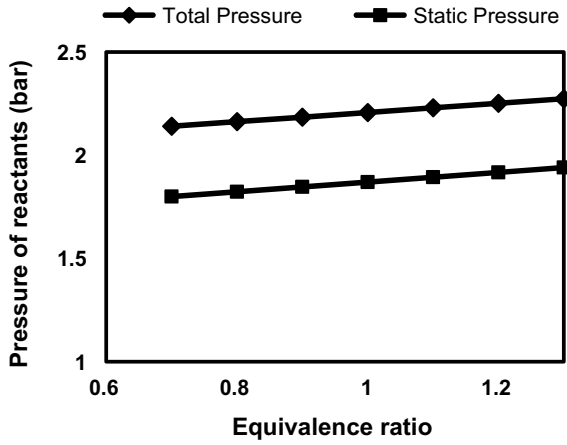
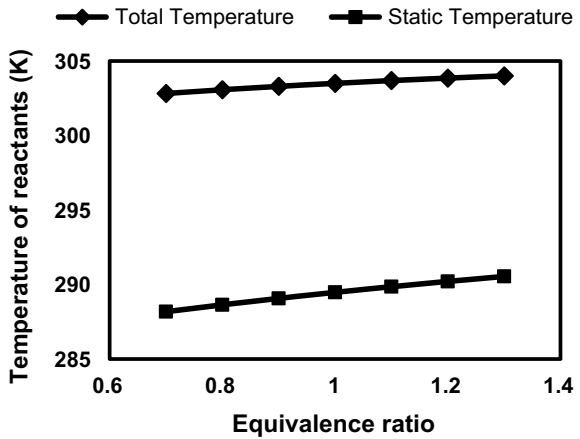


Fig. 8 Total and static temperature of reactants versus equivalence ratio



effect containing low molecular weight hydrogen. Figure 7 shows the distribution of static and stagnation pressures as a function of equivalence ratio. Both of them are almost constant over the equivalence ratios considered. The stagnation value is higher compared to static quantity due to finite Mach number of the flow. Similar trend is seen for the temperatures as shown in Fig. 8.

5 Computation of Detonation Properties

The CJ detonation computations are carried out using the shock and detonation tool box [10] runs in conjunction with Cantera software assuming chemical equilibrium [11]. The quantities of interest are CJ detonation velocity, pressure, temperature and density downstream of detonation wave. Figures 9, 10 and 11 show the CJ detonation velocity, pressure and temperature as a function of fuel-based equivalence ratio. The CJ detonation velocity increases with increase in equivalence ratio. This is due to the increase in sonic velocity of the gases as a result of decrease in molecular weight and increase in temperature. Heat release due to combustion also affects the CJ velocity.

Fig. 9 CJ detonation velocity versus equivalence ratio

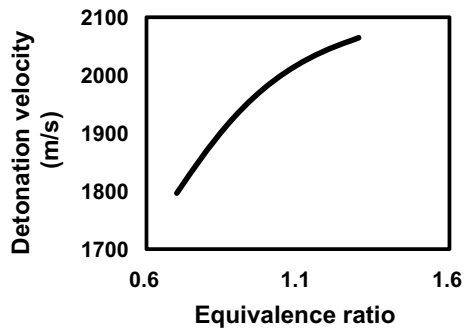


Fig. 10 CJ pressure versus equivalence ratio

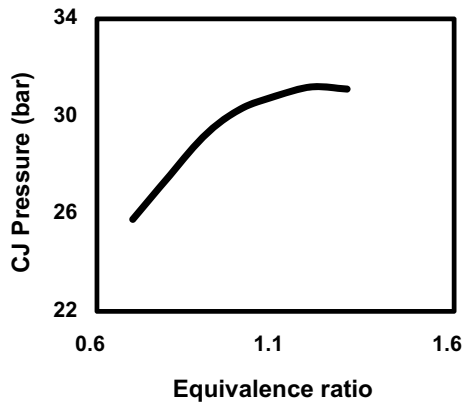
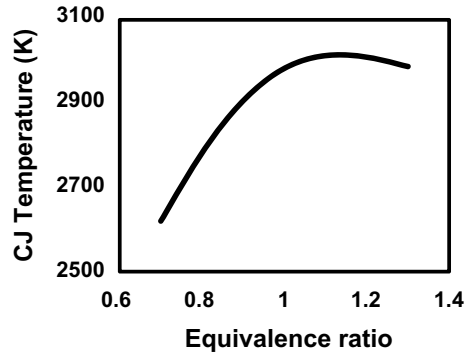


Fig. 11 CJ temperature versus equivalence ratio



Heat release is appreciable as the stoichiometric condition is approached. This in turn increases the CJ pressure and temperature as shown in Figs. 10 and 11. The pressure value becomes almost constant in the fuel excess regime considered in this work. But, the CJ temperature decreases after attaining maximum at stoichiometry.

6 Determination of Averaged Pressure on the Thrust Wall

In order to find the averaged pressure on the thrust wall, one has to model the gas dynamics of the flow field created by the RDE. A simple way is to consider the propagation of the detonation in a layer of height, H over a solid surface. This is equivalent to making an assumption that the flow ahead of the detonation is parallel to the thrust surface, and the detonation wave is normal to the surface. The complex flow field downstream of the detonation wave is shown in Fig. 2. The modelling of the flow field behind the detonation wave is quite complex due to oblique shock wave, contact surface between combustion products of detonation wave and shocked combustion products and the expansion waves. Simplifications reported in literature are utilized to model the above aspects using a self-similar rarefaction wave pressure profile. The flow field was modelled by a few researchers [12] using simple shock solutions and method of characteristics (MOC). Using the data base on rarefaction waves, Sichel and Foster [9] computed impulse function from an infinitely long layer using the parameters, viz., layer height, H and detonation overpressure, ΔP_{CJ} . They gave an expression for pressure along the ground behind detonation wave front. It can be expressed as follows:

$$P(x) - P_{c,1} = (P_{CJ} - P_{c,1})\Psi\left(\frac{x}{H}\right) = \Delta P_{CJ}\Psi(\xi; \gamma_e) \quad (8)$$

The function Ψ depends on the properties of combustion products. The average pressure along the thrust surface is given as follows:

$$\bar{P}_c - P_{c,1} = \Delta P_{CJ} \frac{H}{2\Pi R} \int_0^{2\Pi R/H} \Psi(\xi) d\xi \tag{9}$$

The data of P/P_{CJ} as a function of x/H is curve fitted as a fourth order polynomial (correlation coefficient: 0.99131). The least square fit is given below

$$P/P_{CJ} = -0.0561(x/H)^4 + 0.3455(x/H)^3 - 0.5807(x/H)^2 - 0.153(x/H) + 1.0147 \tag{10}$$

Here, $P/P_{CJ} = \Psi$ and $x/H = \xi$. A few authors have fitted an exponential fit [7] which does not seem to be the best fit to the experimental data. The least square fit for the experimental data is given in Fig. 12 [7]. Using this, the integral term of Eq. 9 can be evaluated to obtain the average pressure on the thrust surface. Figure 13 shows the variation of average pressure as a function of equivalence ratio for hydrogen-air

Fig. 12 Least square fit of experimental data [9]

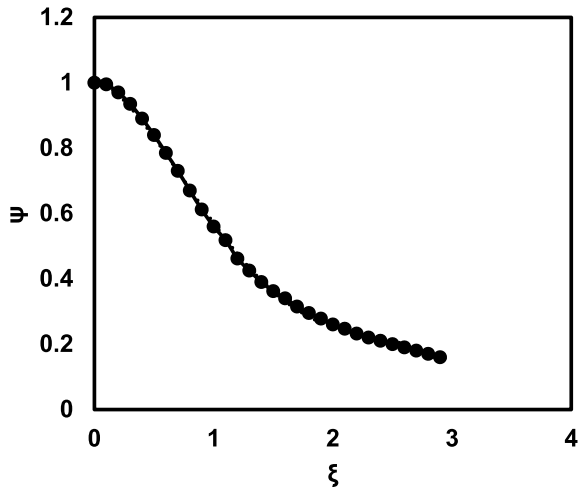
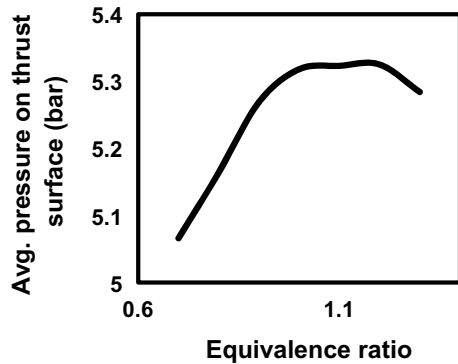


Fig. 13 Average pressure on thrust surface versus equivalence ratio



detonation. The average pressure increases with increase in equivalence ratio due to the strength of the detonation wave as a result of heat release till stoichiometry is reached. Afterwards the pressure value levels off as the fuel rich compositions do not release large energy of combustion. Reduction of pressure is seen for the equivalence ratio of 1.3. The value of detonation layer height, H is shown as a function of equivalence ratio in Fig. 14. The detonation wave height or layer height decreases as the equivalence ratio is increased. This height is inversely proportional to detonation wave velocity for a given mixture flow rate and combustor geometry. The detonation wave velocity increases with increase in equivalence ratio and therefore, the height decreases with increase in equivalence ratio.

Knowing the pressure distribution, the temperature distribution can be evaluated as follows:

$T(x) = T_{CJ} (P(x)/P_{CJ})^{\text{gam}}$ where $\text{gam} = (\gamma - 1)/\gamma$. The pressure and temperature distributions for two detonation cycles at unity equivalence ratio are given in Fig. 15.

Fig. 14 Mixture height versus equivalence ratio

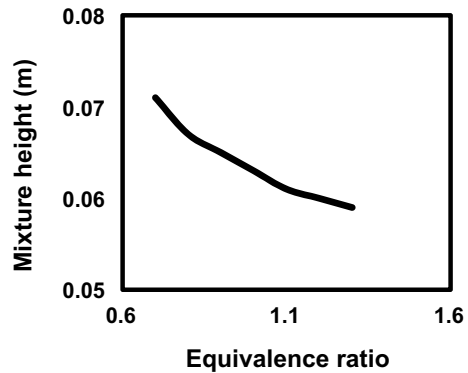
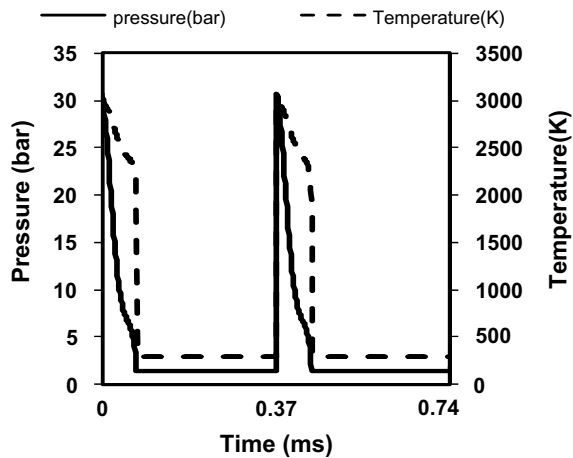


Fig. 15 Pressure and temperature versus time



The starting time ($t = 0$) corresponds to the detonation wave. The pressure and temperature distributions downstream of the detonation wave are shown for two cycles. It is to be seen that the period over which the pressures are in excess of injection static pressure would be the time of blockage of the flow.

The point at which the flow commences until the next detonation cycle getting established can be seen clearly from this detonation cycle diagram based on the downstream expansion waves computed using the experimental least square fit expression explained above. The pressure distributions for varying equivalence ratios of the hydrogen-air detonation are given in Fig. 16. The equivalence ratios are varied from 0.7 to 1.3 to cover either side of the stoichiometry. The value of pressure at the starting point of $x = 0$ is the CJ pressure. The pressure increases with increase in equivalence ratio.

All the pressures merge together after 0.2 m distance from the detonation wave in the circumference of the RDE indicating that the flow of fresh mixture starts entering inside the annular combustor. The corresponding temperature distributions for varying equivalence ratios of the hydrogen-air detonation are given in Fig. 17. In this case, the CJ temperatures are increasing with increasing equivalence ratio

Fig. 16 Pressure versus distance for various equivalence ratios

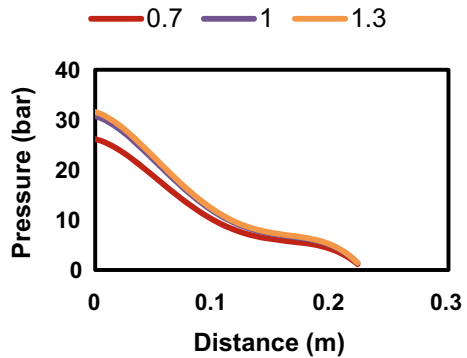
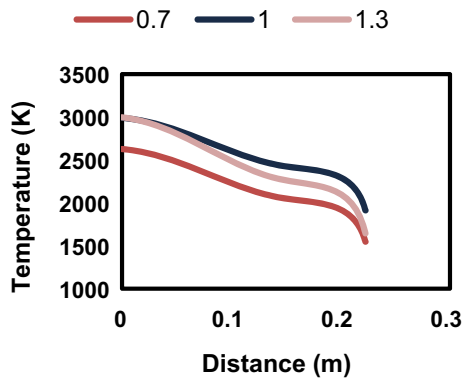


Fig. 17 Temperature versus distance for various equivalence ratios



till stoichiometry. After equivalence ratio equals unity, the temperature starts falling down. The rest of the trend continues as per the distribution function.

7 Propulsion Parameters Under Pressure History Model

Average thrust due to detonation is given by

$$F_I = \Delta P_{CJ} \frac{A_c H}{2 \Pi R} K = \Delta P_{CJ} W H K \tag{11}$$

where K is the value of the integral

$$\text{Thrust}(N) = F_I + F_{II} \tag{12}$$

$$\text{Specific thrust}(N/kg/s) = \text{Thrust}/\text{Total mass flow rate} \tag{13}$$

$$\text{Specific impulse}(s) = \text{Thrust}/(\text{Fuel flow rate} * g) \tag{14}$$

Figure 18 shows the variation of specific thrust with equivalence ratio. The specific thrust increases in the fuel lean regime, attains a maximum at stoichiometry and then decreases in the fuel rich regime. This follows the trend of the average pressure exerted on the thrust surface. However, the numerical values are not very much different over the equivalence ratios considered. Figure 19 shows the variation of fuel-based specific impulse with equivalence ratio. Specific impulse decreases with increase in equivalence ratio due to the increase of fuel flow rate. The fuel-based specific impulse resulted from the present analysis for our configuration using H₂-air is 4733 s compared to a value of 4706 s reported in literature [7] for a stoichiometric composition. The same model has been used to evaluate the C₂H₄-air system. The

Fig. 18 Specific thrust versus equivalence ratio

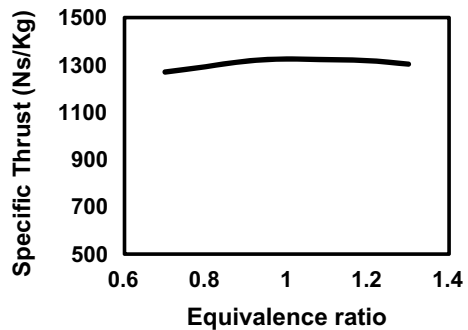
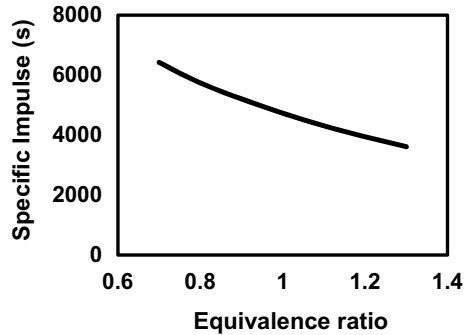


Fig. 19 Specific impulse versus equivalence ratio



specific impulse of our study is 2111 s compared to 1975s reported in literature [7] for the fuel-based equivalence ratio of 0.5.

8 Conclusions

The conclusions of this study are as follows:

1. The objective of obtaining the conditions to be set during the experiments has been fulfilled. The stagnation conditions at the hydrogen fuel and air injection plenum chambers for varying the equivalence ratios over 0.7–1.3 can be set using the flow rates to be handled within the available flow rates of the test facility.
2. As the fuel and oxidiser are injected perpendicular to each other and not injected as a premixed mixture, a simple mixing analysis has been carried out to obtain the conditions ahead of the detonation wave. This was useful in getting the reasonable propulsive performance.
3. The flow properties of detonation wave have been obtained using a well-tested tool box exclusively made for the prediction of shock waves and detonations.
4. The thrust and specific impulse are computed based on “pressure history model” of [7]. This model could yield the performance parameters, which are likely to emerge from the experiments proposed to be conducted at NCCRD, IIT, Madras.
5. The fuel-based specific impulse resulted from the present analysis for our configuration using H_2 -air is 4733 s compared to a value of 4706 s reported [7] for a stoichiometric composition. The same model has been used to evaluate the C_2H_4 -air system. The specific impulse of our study is 2111 s compared to 1975s reported [7] for the fuel-based equivalence ratio of 0.5. These are the reasonable matching values due to certain improvements made in the present study such as incorporation of mixing model and utilizing the curve fit data of the expansion wave pressure decay downstream of the detonation wave in the calculation of average pressure over the porous thrust surface.

6. After obtaining the experimental data, the shortcomings or strength of these simple models can be assessed and corrective actions can be taken using high fidelity models based on CFD.

Acknowledgements The first author expresses his gratitude to CSIR, Government of India for funding the project on RDE under the CSIR Bhatnagar Fellowship Scheme. The support extended by Prof. S. R. Chakravarthy, Coordinator, NCCRD, IIT, Madras for performing the research activities is sincerely acknowledged.

References

1. George AS, Driscoll R, Anand V, Gutmark E (2017) On the existence and multiplicity of rotating detonations. *Proc Combust Inst* 36:2691–2698
2. Yi TH, Lou J, Turangan C, Choi JY, Wolanski P (2011) Propulsive performance of a continuously rotating detonation engine. *J Propul Power* 27(1):171–181
3. Anand V, Gutmark E (2018) Rotating detonations and spinning detonations: similarities and differences. *AIAA J* 56(5):1717–1722
4. Bykovskii FA, Zhdan SA, Vedernikov EF (2006) Continuous spin detonations. *J Propul Power* 22(6):1204–1216
5. Roy RD, Amrutha P, Ramanujachari V (2019) Design of rotating detonation wave combustor based on detonation cell width correlations. In: *Proceedings, 26th national conference on internal combustion engines and combustion*, NIT Kurukshetra, India
6. Davidenko DM, Eude Y, Gokalp I, Falempin F (2011) Theoretical and numerical studies on continuous detonation wave engines. In: *AIAA 2011–2334*
7. Shepherd JE, Kasahara J (2017) Analytical models for the thrust of a rotating detonation engine. *GALCIT Report*, CIT, CA, USA
8. Braun EM (2012) New detonation concepts for propulsion and power generation. PhD Thesis, University of Texas at Arlington, USA
9. Sichel M, Foster JC (1979) The ground impulse generated by a plane fuel air explosion with side relief. *Acta Astronaut* 6:243–256
10. Browne S, Ziegler J, Shepherd JE (2008) Numerical solution method for shock and detonation jump conditions. *GALCIT Report FM 2006.006*
11. Goodwin D (2010) Cantera: object oriented software for reactive flows. <http://code.google.com/p/cantera>
12. Fievisohn RT, Yu KH (2016) Steady state analysis of rotating detonation engine flow fields with method of characteristics. *J Propul Power*, online publication, Article in Advance